Epigenetic Regulation of Foxp3 Expression in Regulatory T Cells by DNA Methylation[1]

Girdhari Lal,* Nan Zhang,* William van der Touw,* Yaozhong Ding,*†‡§ Wenjun Ju,¶ Erwin P. Bottinger,¶ St. Patrick Reid,‖ David E. Levy,‖ and Jonathan S. Bromberg[2]*†‡§

Foxp3, a winged-helix family transcription factor, serves as the master switch for CD4$^+$ regulatory T cells (Treg). We identified a unique and evolutionarily conserved CpG-rich island of the *Foxp3* nonintronic upstream enhancer and discovered that a specific site within it was unmethylated in natural Treg (nTreg) but heavily methylated in naive CD4$^+$ T cells, activated CD4$^+$ T cells, and peripheral TGFβ-induced Treg in which it was bound by DNMT1, DNMT3b, MeCP2, and MBD2. Demethylation of this CpG site using the DNA methyltransferase inhibitor 5-aza-2′-deoxycytidine (Aza) induced acetylation of histone 3, interaction with TIEG1 and Sp1, and resulted in strong and stable induction of Foxp3. Conversely, IL-6 resulted in methylation of this site and repression of Foxp3 expression. Aza plus TGFβ-induced Treg resembled nTreg, expressing similar receptors, cytokines, and stable suppressive activity. Strong Foxp3 expression and suppressor activity could be induced in a variety of T cells, including human CD4$^+$CD25$^-$ T cells. Epigenetic regulation of *Foxp3* can be predictably controlled with DNMT inhibitors to generate functional, stable, and specific Treg. ***The Journal of Immunology,*** **2009, 182: 259–273.**

Regulatory T cells (Treg)[3] play important roles in many different immune responses (1–3). Foxp3 is the major transcription factor that determines the fate and identity of Treg, and it is expressed in the thymus in natural Treg (nTreg) (4, 5). Signals important for induction of *Foxp3* include IL-2 and TCR (6), and these influence *Foxp3* promoter structure (7, 8). Foxp3 can also be induced in peripheral naive CD4$^+$CD25$^-$ T cells by TGFβ (9, 10). Transient expression of Foxp3 in peripheral CD4$^+$ T cells induces suppressive characteristics (11), but constitutive expression as in nTreg is required for stable suppressive function (12). Numerous protocols using a variety of APCs and cytokine signals, particularly TGFβ, have been developed to induce peripheral Treg (13); however, the strength and stability of Foxp3 expression is variable. Thus, therapeutic use of Treg requires a better understanding of signals that regulate Foxp3 expression to convert naive T cells to Treg, perhaps recapitulating intrathymic rather than peripheral regulation of Foxp3 expression.

Epigenetic regulation by methylation of 5′-cytosine of CpG dinucleotides regulates gene expression and development of cell lineages. CpG methylation of the promoter down-regulates transcription by preventing the binding of positive transcription factors to their recognition sequences and by recruiting repressor molecules, such as the methyl-binding proteins MBD, MeCP1, MeCP2, and DNA methyltransferases (DNMTs) (14). Methyl-binding proteins share homologous regions termed transcription repressor domains, recruit histone deacetylases (HDACs) and the factors that regulate them, and repress open chromatin configurations (15). Recently, it has been shown that there is an intronic enhancer of *Foxp3* with CpG residues that are differentially methylated and that possesses functional CREB and activating transcription factor (ATF) sites (7, 16–18). In addition there is another contiguous intronic enhancer without CpG sites that has functional NFAT and Smad3 binding sites (19). These findings suggest a model in which TGFβ- and TCR-initiated signals synergize to activate transcription. Other than these intronic regions, the *cis*-elements and signals that regulate them for constitutive *Foxp3* expression and development of nTreg are not well understood. Because the regulatory elements for the development of Th1 and Th2 cells are spread along the chromosome to form cell lineage-specific loci (20–22), and a number of these important regulatory units are epigenetically regulated (23–25), it is likely that there are other important upstream regions for the regulation of *Foxp3* and Treg.

In the present study, we examined ~30 kb of genomic DNA and demonstrated that a highly conserved, nonintronic, upstream enhancer contained a CpG island with a specific site that recruited MeCP2, MBD2, DNMT1, and DNMT3b and was methylated in peripheral CD4$^+$ T cells, but not in nTreg. The chromatin in this region was histone H3 acetylated and bound by Sp1 and TGFβ-inducible early gene-1 (TIEG1) in nTreg but not in naive CD4$^+$CD25$^-$ T cells and, importantly, not in peripheral TGFβ-induced Treg, showing that nTreg and TGFβ-induced Treg enhancers are structurally distinct. This upstream Foxp3 enhancer was demethylated and activated by the DNMT inhibitor 5-aza-2′-deoxycytidine (Aza), leading to strong Foxp3 expression in CD4$^+$CD25$^-$ T cells. Conversely, IL-6 caused methylation of this site and repression of Foxp3 expression. The combination of Aza plus TGFβ synergistically induced highly enriched CD4$^+$CD25$^+$

*Department of Gene and Cell Medicine, †Department of Surgery, ‡Recanati/Miller Transplantation Institute, §Immunology Center, and ¶Department of Medicine, Mount Sinai School of Medicine, New York, NY 10029; and ‖Department of Pathology and Microbiology, New York University School of Medicine, New York, NY 10016

Received for publication August 15, 2008. Accepted for publication October 22, 2008.

The costs of publication of this article were defrayed in part by the payment of page charges. This article must therefore be hereby marked *advertisement* in accordance with 18 U.S.C. Section 1734 solely to indicate this fact.

[1] This work was supported by National Institute of Health Grants AI41428 and AI62765 and Juvenile Diabetes Research Foundation Grant 1-2005-16 (all to J.S.B.).

[2] Address correspondence and reprint requests to Dr. Jonathan S. Bromberg, Mount Sinai School of Medicine, One Gustave L. Levy Place, Box 1104, New York, NY 10029-6574. E-mail address: Jon.Bromberg@mountsinai.org

[3] Abbreviations used in this paper: Treg, regulatory T cell; AcH3, acetylated histone 3; AID, activation-induced cytidine deaminase; ATF, activating transcription factor; Aza, 5-aza-2′-deoxycytidine; ChIP, chromatin immunoprecipitation; DNMT, DNA methyltransferase; EGR1, early growth response 1; HDAC, histone deacetylase; nTreg, natural Treg; qRT-PCR, quantitative RT-PCR; TIEG1, TGFβ-inducible early gene-1.

Foxp3$^+$ T cells that were genetically and functionally stable and suppressive. Foxp3 expression and suppressive activity could be induced in human CD4$^+$CD25$^-$ T cells. The results have important implications for delineating T cell development and differentiation, generating Treg for clinical use, and understanding the consequence of epigenetic regulation for immunity.

Materials and Methods

Antibodies and reagents

Aza and RG108 were from Calbiochem. Hydralazine and procainamide were purchased from Sigma-Aldrich. Recombinant purified mouse IL-2, recombinant human IL-2, recombinant purified mouse IL-4, recombinant mouse IL-6, recombinant mouse IL-12, recombinant purified IFN-γ, recombinant human TGFβ1, functional grade purified anti-mouse CD3ε (145-2C11), functional grade purified anti-human CD3ε (OKT3), functional grade purified anti-mouse IL-4 (11B11), FITC anti-human CD25 (BC96), allophycocyanin anti-human CD4 (OKT4), allophycocyanin anti-mouse CD4 (GK1.5), PE anti-mouse CD8 (53-6.7), FITC anti-mouse CD25 (PC61.5), PE anti-mouse CD62L (MEL-14), PE anti-mouse CD44 (IM7), PE anti-mouse CD45RB (C363.16A), PE anti-mouse CD45.1 (A20), PE anti-mouse CD69 (H1.2F3), PE anti-mouse CTLA4 (UC10.4B9), PE anti-mouse CD127 (A7R34), PE anti-mouse CD122 (5H4), PE anti-mouse CD28 (37.51), PE anti-mouse CD253 (N2B2), and PE anti-mouse/rat Foxp3 (FKJ-16s) Abs and isotype control Abs were purchased from eBioscience. Functional grade purified anti-mouse IFN-γ (XMG1.2) Ab was purchased from BD Pharmingen. Mouse anti-Sp1 (1C6), rabbit anti-mouse acetylated histone H3 (Lys 9/14), rabbit anti-mouse pSmad2/3 (Ser$^{433/435}$), rabbit anti-DNMT1 (H-300), rabbit anti-DNMT3a (H295), and mouse anti-DNMT3b (52A1018), anti-TIEG1 (H-190), anti-MBD2 (N-18), anti-MeCP2 (H-300), anti-early growth response 1 (EGR1) (H-250), and anti-AP-2α (3B5) Abs and control Abs were purchased from Santa Cruz Biotechnology. Anti-TGFβ1, β2, and β3 mAbs (1D11) were purchased from R&D Systems. CFSE and an annexin-V staining kit were purchased from Invitrogen. pGFP-DNMT1, pGFP-DNMT3a, and pGFP-DNMT3b1 constructs were provided by Dr. H. Leonhardt, Biozentrum der Ludwig-Maximilians-Universität, Planegg-Martinsried, Germany.

Mice

BALB/c, C57BL/6, CD45.1 congenic C57BL/6, and CB.17 SCID 8- to 10-wk-old mice were purchased from The Jackson Laboratory. Foxp3gfp reporter mice were provided by A.Y. Rudensky (University of Washington, Seattle, WA) and maintained in our facility. Smad3$^{-/-}$ and STAT3$^{-/-}$ (CD4 Cre:STAT3 f/f) mice were maintained in our facilities (26, 27). All mice were housed in a specific pathogen-free facility in microisolator cages. All experiments used age- and sex-matched mice in accordance with protocols approved by the Mount Sinai School of Medicine Institutional Animal Care and Utilization Committee.

Purification and culture of mouse T cells

Mice were sacrificed, spleens were removed and gently dissociated into single cell suspensions, and RBC were removed using hypotonic ACK (ammonium chloride potassium) lysis buffer. Splenocytes were enriched for CD4$^+$ T cells using a CD4$^+$ negative selection kit (R&D Systems). Cells were stained with allophycocyanin anti-mouse CD4, PE anti-mouse CD8, and FITC anti-mouse CD25 Abs for 30 min on ice. CD4$^+$CD25$^-$ cells and CD4$^+$CD25$^+$ cells were sorted using FACSVantage DiVa (BD Bioscience) or MoFlo (DakoCytomation). The purity of cells was >99%. T cell-depleted splenocytes were used as stimulator cells (APC). Purified CD4$^+$CD25$^-$ T cells (5×10^4 cells/well) were cultured with gamma-irradiated (800 rad), syngeneic, T cell-depleted splenocytes (5×10^4 cells/well) in the presence of IL-2 (10 ng/ml), anti-CD3ε mAb (1 μg/ml), TGFβ (5 ng/ml) and Aza (0.04–10 μM) or RG108 (5 μM), hydralazine (5 μM), or procainamide (5 μM) in a final volume of 200 μl of complete RPMI medium (RPMI 1640 supplemented with 10% FBS, 1 mM sodium pyruvate, 2 mM L-glutamine, 100 IU/ml penicillin, 100 μg/ml streptomycin, 1× nonessential amino acids, and 2×10^{-5} M 2-ME) in U-bottom 96-well plates (Corning). Cells were cultured for the indicated number of days at 37°C in a 5% CO_2 incubator. Anti-TGFβ mAb (10 μg/ml) was added to neutralize serum TGFβ. For Th1 conditions, IL-12 (5 ng/ml), IFN-γ (20 ng/ml), and anti-IL-4 (10 μg/ml) were added in culture. For Th2 conditions, IL-4 (10 ng/ml) and anti-IFN-γ (10 μg/ml) were added in culture. For Th17 conditions, IL-6 (10 ng/ml) and TGFβ (5 ng/ml) were used in culture.

Cell staining and flow cytometric analysis

Staining was performed with the specific Ab (1 μg/10^6 cells) at 4°C for 30 min. Cells were analyzed using the FACSCalibur flow cytometer using CellQuest software (BD Biosciences). Data were analyzed using FlowJo software (Tree Star).

Human lymphocyte purification and culture

CD4$^+$CD25$^-$ and CD4$^+$CD25$^+$ T cells were purified from peripheral blood of healthy individuals. Detailed purification and culture conditions of human T cell are given in the supplemental *Materials and Methods*.[4]

Quantitative real-time RT PCR (qRT-PCR)

Total RNA purification and qRT-PCR are described in the supplemental *Materials and Methods*.

Chromatin immunoprecipitation (ChIP) assay

ChIP assay was performed using the ChIP kit (Upstate). The immunoprecipitated DNA was amplified by real-time PCR. DNA enrichment was calculated with the equation $2^{[\text{DNAinput}] - [\text{DNAspecificIP}]/[\text{DNAinput}] - [\text{DNAnonspecificIP}]}$, where [DNAspecificIP] is the amount of the DNA immunoprecipitated using the Ab of interest, [DNAnonspecificIP] is the amount of DNA immunoprecipitated by a nonspecific control Ab, and [DNAinput] was an aliquot of sheared chromatin sample before immunoprecipitation and was used to normalize the sample to the amount of chromatin added to each ChIP. The primers used for the upstream *Foxp3* enhancer CpG site were 5′-GCGGAGAGGGATCGGGAAA-3′ (forward) and 5′-ATGAGGAAGACGATGGCGAGGAT-3′ (reverse), and the primers for the *Foxp3* proximal promoter were 5′-CCTTGGCAACATGATGGTGGTGAT-3′ (forward) and 5′-AAGAAGGGATCAGAAGCCTGCCAT-3′ (reverse).

PCR-based assay for enhancer methylation

A methyl-sensitive PCR was used to analyze the methylation status of the CpG island of the Foxp3 promoter. Genomic DNA was prepared using a blood DNA extraction kit (Qiagen). One microgram of genomic DNA isolated from the indicated T cells was digested with 10 U of *Hpa*II or *Msp*I enzymes overnight at 37°C. The Foxp3 CpG island and *H19* were PCR amplified using the following specific primers: Foxp3 enhancer CpG island, 5′-ATCCTCGCCATCGTCTTCCTCAT-3′ (forward) and 5′-CCTGTTCTGGCTTTCTCATTGGCT-3′ (reverse); *H19* (GenBank accession no. U19619.1), 5′-AATTGGGGCGTTCAGATGCTAATG-3′ (forward) and 5′-TTTCTGGCATCGAACCACATGCAC-3′ (reverse); activation-induced cytidine deaminase (*AID*) (Ensembl gene identifier ENSMUSG00000040627), 5′-CCACCCTCTGCTCAGGTCTTTTGGG-3′ (forward) and 5′-ATGTTGGATATTTGCCAAATAATTG-3′ (reverse). PCR consisted of an initial denaturation of 95°C for 15 min, followed by 35 cycles of 95°C for 30s, 55°C for 30s, and 72°C for 30s. The PCR products were analyzed on 2% agarose gels, stained with ethidium bromide, and photographed.

Disulfite sequencing

Genomic DNA was prepared using the blood DNA extraction kit (Qiagen). DNA was denatured, modified with sodium metabisulfite, purified, and desulfonated using a CpGenome Fast DNA modification kit (Chemicon International). Disulfite primers were designed using MethPrimer software (www.urogene.org/cgi-bin/methprimer/methprimer.cgi). *Foxp3* enhancer CpG island from −5782 to −5558 was PCR amplified using 5′-AATGTGGGTATTAGGTAAAATTTTT-3′ (forward) and 5′-AAACCCTAAAACTACC TCTAAC-3′ (reverse) primers. *Foxp3* CpG island from −5252 to −5030 was PCR amplified using 5′-TAGGTGATTGATAAGTAGGAGAAGTTAGTA-3′ (forward) and 5′-TACCCCCATTACTTATAACCATTTC-3′ (reverse) primers. *H19* was amplified using 5′-AGTATTTTAGGGGGGTTATAAATG-3′ (forward) and 5′-ACCCATAACTATAAAATCATAAA-3′ (reverse). PCR products were separated on agarose gels, excised, and cloned into the pGEM-T easy vector (Promega). Recombinant plasmid DNA from the individual bacterial colonies were purified and sequenced.

EMSA

Nuclear extracts were made using a nuclear extraction kit (Novagen). EMSA assays were performed with 10 μg of nuclear extract and 5′-biotinylated Foxp3 CpG enhancer oligonucleotides using a LightShift Chemiluminescent EMSA kit (Pierce). The DNA-protein complex was resolved

[4] The online version of this article contains supplemental material.

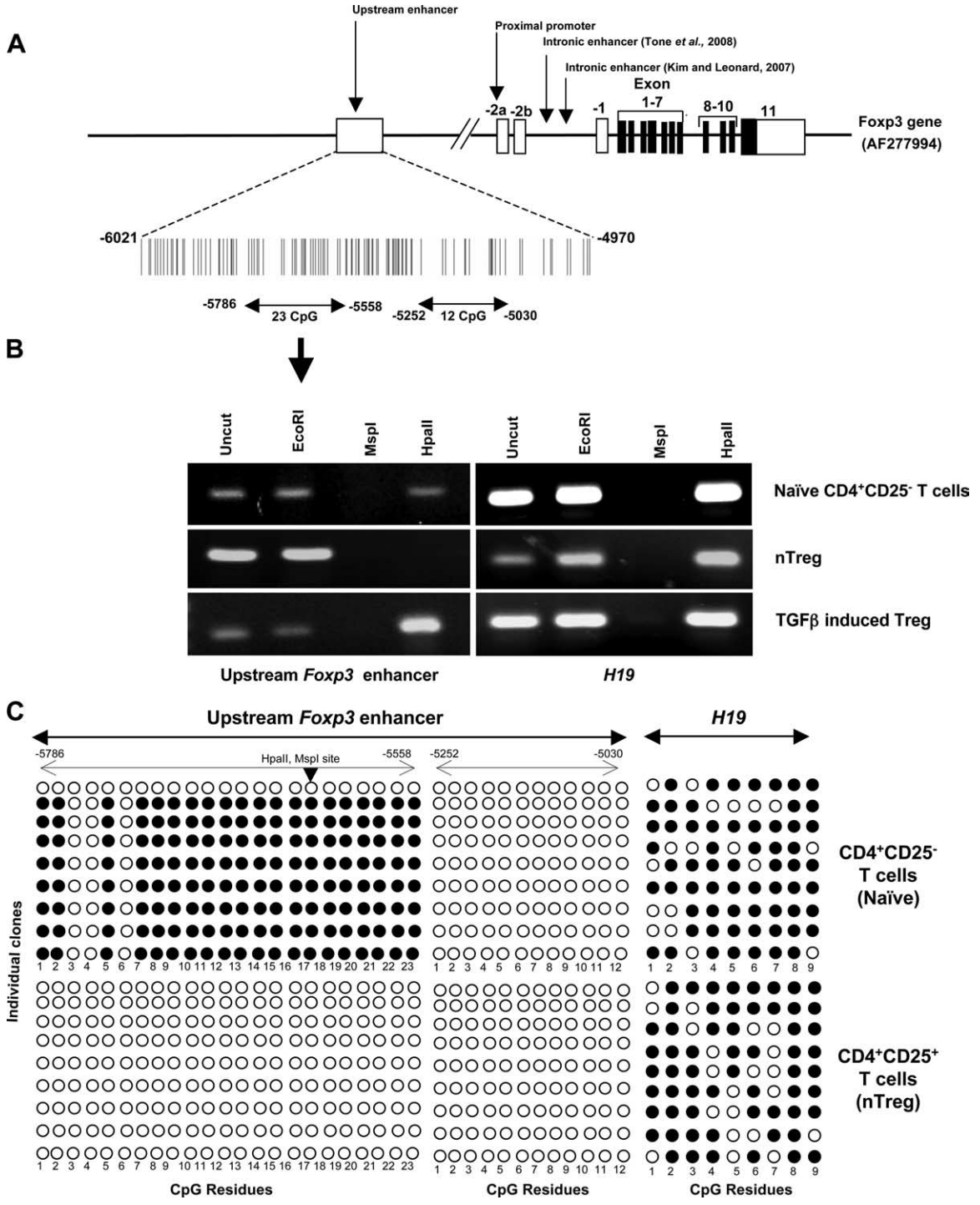

FIGURE 1. Methylation of upstream Foxp3 CpG island. *A*, Schematic view of mouse *Foxp3* gene and upstream CpG island analyzed with GrailExp software (compbio.ornl.gov). Filled bars represent the individual CpG residues. "Kim and Leonard, 2007" is Ref. 7 and "Tone et al., 2008" is Ref. 19. *B*, $CD4^+CD25^-gfp^-$ T cells (naive) and $CD4^+CD25^+gfp^+$ T cells (nTreg) were purified. $CD4^+CD25^-gfp^-$ T cells were cultured with irradiated, syngeneic, T cell-depleted splenocytes in the presence of IL-2, anti-CD3ε mAb, and TGFβ for 4 days, and $CD4^+CD25^+gfp^+$ T cells were purified by FACS sorting. Genomic DNA was isolated, digested with *Msp*I (methyl insensitive), *Hpa*II (methyl sensitive), or *Eco*RI (negative control), PCR amplified using upstream Foxp3 enhancer- or *H19*-specific primers, and PCR products were resolved on agarose gels. Data are representative of three experiments. *C*, Genomic DNA was isolated from the indicated T cell subsets, modified with sodium bisulfite, PCR amplified, cloned into the pGEM-T vector, and individual clones were sequenced. The methylation pattern of each clone obtained is shown. ●, Methylated CpG; ○, nonmethylated CpG.

by PAGE on 4% polyacrylamide nondenaturing gel. The 5′-biotin-labeled Foxp3 enhancer CpG oligo sequence 5′- TGCCCGCCCCGGGCCCGCCC CACGGCCGGTAGCGGCGTAC-3′ was synthesized by Sigma-Genosys. Sp1 consensus oligonucleotide (5′-ATTCGATCGGGGCGGGGCGAGC-3′) was purchased from Promega.

Construction of luciferase vector

Genomic DNA was purified from naive $CD4^+CD25^-$ T cells. Foxp3 enhancer (352 bp) was amplified using the specific primers 5′-CGGGGTA CCATCCTCGCCATCGTCTTCCTCAT-3′ (forward) and 5′-GAAGATC

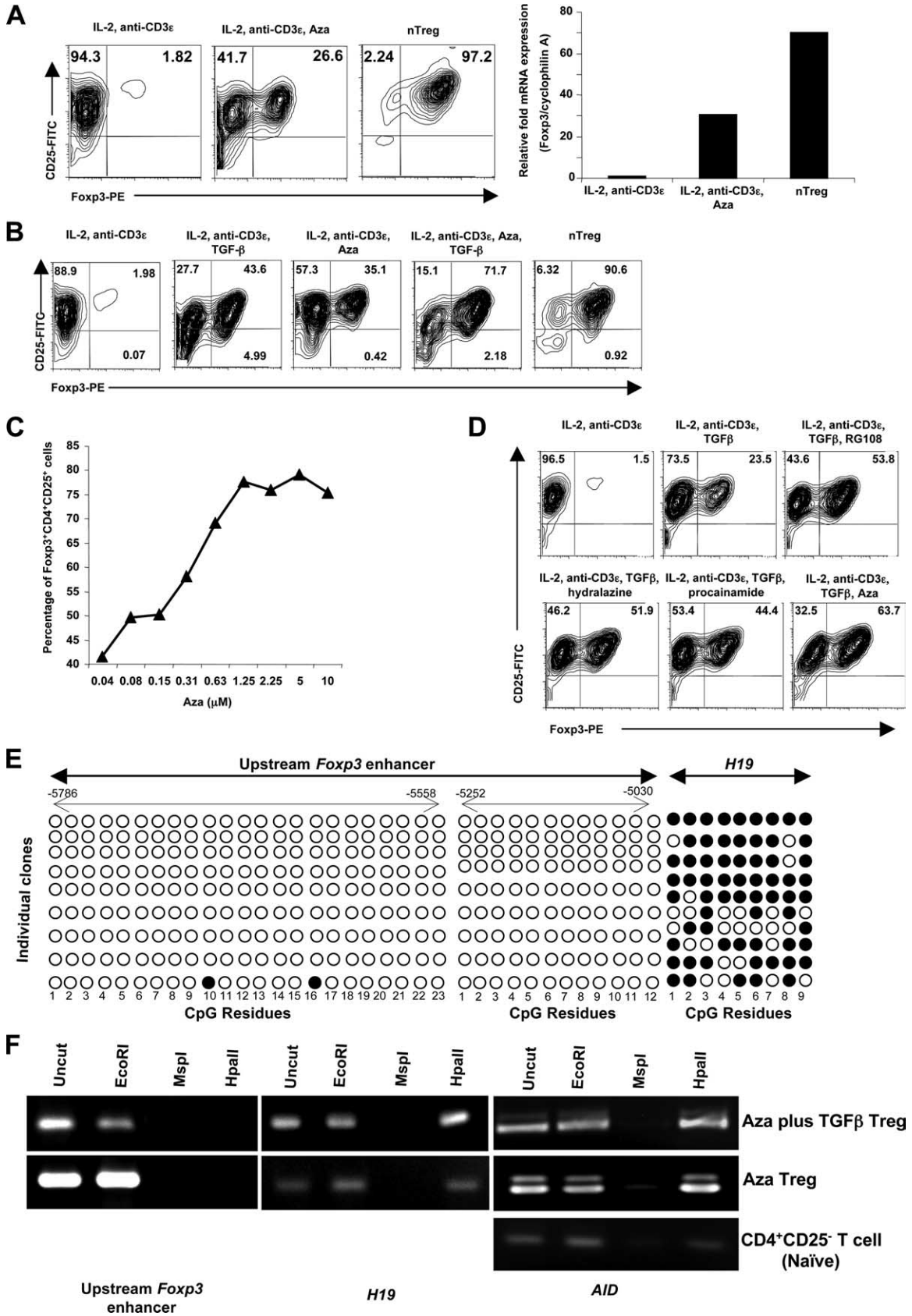

FIGURE 2. DNMT inhibitors induce Foxp3 expression in $CD4^+CD25^-$T cells. *A*, $CD4^+CD25^-$ T cells from BALB/c male mice were cultured with irradiated, syngeneic, T cell-depleted splenocytes in the presence of IL-2 (10 ng/ml), anti-CD3ε mAb (1 μg/ml), or Aza (10 μM) for 4 days. nTreg were cultured without Aza. Intracellular Foxp3 was analyzed by gating on $CD4^+$ cells (*left*). Foxp3 mRNA expression in the same cultured cells was analyzed by qRT-PCR (*right*). *B*, $CD4^+CD25^-$ T cells from BALB/c male mice were cultured for 4 days in the presence of IL-2, anti-CD3ε, TGFβ, and Aza (10 μM). Intracellular Foxp3 was analyzed by gating on $CD4^+$ cells. *C*, Dose response to Aza for Foxp3 expression in $CD4^+CD25^-$ T cells in the presence of IL-2, anti-CD3ε mAb, and TGFβ. *D*, Foxp3 expression in $CD4^+CD25^-$ cells cultured in the indicated conditions along with the DNMT inhibitors

TTGTTCTGGCTTTCTCATTGGCTGC-3′ (reverse). Amplified PCR product was cloned into the *Kpn*I and *Bgl*II sites of the pGL3 promoter vector (Promega) proximal to minimal SV40 promoter to generate pGL3-CpG plasmid. The BW5147.3 cell line, a mouse T cell lymphoma, was purchased from the American Type Culture Collection. BW5147.3 (1×10^6 cells) were transfected with the pGL3 promoter vector or the pGL3-CpG plasmid (3.0 μg) using a TransFast transfection reagent (Promega). Synthetic *Renilla* luciferase reporter vector (pRL-TK, 0.3 μg; Promega) was used as internal control for transfection efficiency. Forty-eight hours after transfection, cells were harvested and luciferase activity was measured using a Dual luciferase assay system (Promega). Data were normalized to the *Renilla* luciferase activity.

For in vitro methylation, the upstream *Foxp3* enhancer was excised from the pGL3-CpG plasmid with *Kpn*I and *Bgl*II, isolated by gel elution, and in vitro methylated using *Sss*I methylase (New England Biolabs). DNA methylation was verified using *Hpa*II, a methylation-sensitive restriction enzyme. The methylated enhancer was religated into the pGL3-promoter, the ligated DNA (3 μg) was transfected into the BW5147.3 cell line, and luciferase activity was monitored as described above.

Proliferation and suppression assays

Flow cytometrically purified $CD4^+CD25^-$ T cells were labeled with CFSE (5 μM) for 5 min at 37°C. CFSE-labeled $CD4^+CD25^-$ T cells (5×10^4 cells/well) were cultured in the presence or absence of Treg (5×10^4 cells/well) with irradiated (800 rad) syngenic T cell-depleted splenocytes (5×10^4 cells/well) and anti-CD3ε mAb (1 μg/ml) for 3 days. Cells were harvested and CFSE dilution was analyzed using a LSR II flow cytometer (BD Biosciences) or a FACSCalibur cytometer (BD Biosciences). Human suppression assay is described in the supplemental *Materials and Methods*.

Islet transplantation and colitis

Allogenic islet transplantation and induction of colitis in SCID mice are described in the supplemental *Materials and Methods*.

Statistical analysis

Values are given as mean of the individual sample ± SD. Statistical significance was assessed using Student's *t* test. Difference of graft survival times was assessed by Kaplan-Meier survival analysis with StatView software. $p < 0.05$ is considered statistically significant.

Results

Methylation of upstream Foxp3 enhancer

Analysis of ~30 kb of mouse genomic DNA containing the *Foxp3* gene (GenBank accession no. AF277994) demonstrated that upstream to the transcriptional start site is a CpG island at −4970 to −6021 with 66.95% GC and an observed:expected GC ratio of 0.92 (Fig. 1*A*), and this sequence is highly conserved in humans (92% identity) (supplemental Fig. S1). Its methylation status was determined by methyl-specific restriction digestion. Because *Foxp3* is on the X-chromosome, male mice cells were used to avoid artifacts from X-chromosome inactivation in females. To ensure highly purified cells, Foxp3gfp mice were used (5). The site from residues −5786 to −5558 containing 23 CpG was methylated in naive $CD4^+CD25^-gfp^-$ T cells but demethylated in $CD4^+CD25^+Foxp3^+gfp^+$ nTreg (Fig. 1*B*). In TGFβ induced $CD4^+CD25^+Foxp3^+gfp^+$ Treg this site was also methylated (Fig. 1*B*), demonstrating significant differences in the genomic structure of the two Treg subsets. The *H19* gene used as a control is demethylated and expressed during gametogenesis and is methylated in differentiated T cells (28). *H19* was methylated in all T cell subsets tested (Fig. 1*B*) so that DNA demethylation was upstream *Foxp3* enhancer specific. Disulphite sequencing also showed that the upstream *Foxp3* enhancer was heavily methylated (~90%) in naive $CD4^+$ T cells but completely demethylated in nTreg (Fig. 1*C*). A different nearby site from −5252 to −5030 containing 12 CpG was demethylated in all T cell subsets (Fig. 1*C*). The *H19* control region was methylated in both naive and nTregs (Fig. 1*C*). Together, these results demonstrated a specific upstream *Foxp3* CpG site in the *Foxp3* enhancer that was similarly methylated in naive $CD4^+$ T cells and TGFβ-induced peripheral Treg, but demethylated in nTreg.

Demethylation of upstream Foxp3 enhancer induces Foxp3 expression

Because there was differential methylation of the upstream *Foxp3* enhancer in T cell subsets, we determined whether the site could be demethylated and Foxp3 expression induced with the DNMT inhibitor Aza, an anticancer drug known as decitabine, that can induce the expression of methylated genes (29). Aza induced Foxp3 protein and mRNA expression in naive $CD4^+CD25^-$ T cells (Fig. 2*A*) in a dose- (supplemental Fig. S2*A*) and time-dependent fashion (supplemental Fig. S2, *B* and *C*). The addition of anti-TGFβ mAb to culture did not inhibit Aza-induced Foxp3 expression, showing that serum TGFβ was not required for Aza to inhibit DNMTs (not shown). Further, whereas TGFβ induces Foxp3 expression in peripheral naive $CD4^+CD25^-$ T cells (9, 10), the results in Fig. 1*B* showed that the upstream Foxp3 enhancer remained methylated in TGFβ-induced Treg. Because TGFβ does induce Foxp3, the combination of Aza plus TGFβ was tested for Foxp3 induction. The results showed that Aza plus TGFβ efficiently induced Foxp3 in 72% of T cells compared with 44% with TGFβ alone, 35% with Aza alone, and 91% in control nTreg (Fig. 2*B*). This effect was synergistic, so that expression was induced by even very low concentrations of Aza plus TGFβ (Fig. 2*C*) compared with Aza alone (supplemental Fig. S2*A*). The other mechanistically and structurally diverse DNMT inhibitors RG108, hydralazine, and procainamide also induced Foxp3 expression in combination with TGFβ (Fig. 2*D*). Importantly, in our culture conditions Aza or Aza plus TGFβ lead to complete demethylation of the *Foxp3* CpG site, whereas the *H19* promoter and *AID* first intronic region remained methylated (Fig. 2, *E* and *F*). The *AID* intronic region has been shown to be hypomethylated in germinal center B cells but hypermethylated and not expressed in T cells (30).

Aza plus TGFβ-induced Treg expressed similar levels of cytokine mRNA except for slightly increased IL-4 and IL-17 mRNA and a greater increase in IL-10 mRNA compared with nTreg (supplemental Fig. S2*D*), and expressed similar surface markers, except for slight decreases in CD28, CD62L, and CD122 (IL-2Rβ) (supplemental Fig. S2*E*). Thus, Aza induced demethylation of the upstream *Foxp3* enhancer to allow enhanced Foxp3 expression and subsequent downstream effects of induction of Foxp3-dependent, Treg-restricted sets of genes

RG108 (5 μM), hydralazine (5 μM), procainamide (5 μM) or Aza (5 μM). Inhibitors were removed after 24 h and cells were recultured for another 3 days. Foxp3 expression was analyzed by gating on $CD4^+$ cells. *E*, $CD4^+CD25^-$ $Foxp3gfp^-$ T cells were purified from Foxp3gfp reporter male mouse spleens using flow cytometry. $CD4^+CD25^-Foxp3gfp^-$ (50,000 cells/well) were cultured with irradiated T cell-depleted syngenic splenocytes (50,000 cells/well) along with IL-2, anti-CD3ε, TGFβ, and Aza for up to 4 days. Aza was removed after 24 h. $CD4^+CD25^+Foxp3gfp^+$ T cells were purified by flow cytometry after culture. Methylation of upstream *Foxp3* enhancer CpG island and *H19* in TGFβ plus Aza-induced $CD4^+CD25^+Foxp3^+gfp^+$ Treg was analyzed by disulfite sequencing. *F*, Methyl-specific restriction digestion of genomic DNA and PCR analysis of upstream *Foxp3* enhancer, *H19*, and the first intronic region of *AID* in Aza- and Aza plus TGFβ-induced $CD4^+CD25^+Foxp3^+gfp^+$ Treg. Data are representative of 2–4 independent experiments for each panel.

rather than indiscriminately activating many loci. Together, these results showed that Aza plus TGFβ-induced Treg were similar to conventional nTreg.

Upstream Foxp3 enhancer is occupied by DNMTs and transcriptional repressors

DNA methylation is performed by three known DNMTs: DNMT1, DNMT3a, and DNMT3b. ChIP assays for DNMTs showed that nTreg had >8-fold difference in DNMT1 and >12-fold difference in DNMT3b binding to the upstream Foxp3 enhancer CpG island compared with naive $CD4^+$ T cells (Fig. 3*A*), whereas there was no significant difference in DNMT3a binding (supplemental Fig. S3). The results for Aza plus TGFβ Treg were similar to those of nTreg. Importantly, TGFβ-induced Treg had much greater binding of DNMT1 and DNMT3b compared with nTreg or Aza plus TGFβ-induced Treg (Fig. 3*A*). This suggested that DNMT1 and DNMT3b were recruited to the upstream *Foxp3* enhancer to maintain CpG methylation in naive $CD4^+$ T cells and TGFβ-induced Treg. There was similar differential binding of the transcriptional repressors MBD2 and MeCP2 to this same site in naive $CD4^+CD25^-$ T cells, activated T cells, and TGFβ-induced Treg compared with Aza plus TGFβ-induced Treg or nTreg (Fig. 3, *B* and *C*).

To further assess the upstream *Foxp3* enhancer activity, the sequence was cloned into a vector with an SV40 minimal promoter and luciferase reporter activity was measured after transfection into the BW5147.3 T cell lymphoma line. This upstream *Foxp3* enhancer induced ~30-fold reporter activity compared with the control vector (Fig. 3*D*). Cotransfection of DNMT1, DNMT3a, or DNMT3b1 inhibited enhancer activity, suggesting that methylation repressed transcriptional activity (Fig. 3*E*). To demonstrate that inhibition of enhancer activity was due to methylation of the enhancer and not the vector backbone, the upstream *Foxp3* enhancer was first methylated in vitro, ligated into the pGL3 promoter vector, and then enhancer activity was monitored after transfection into the BW5147.3 cell line. The results show that in vitro methylation inhibits upstream Foxp3 enhancer activity (Fig. 3*F*).

Sp1 and TIEG1 binding and histone 3 acetylation in Treg subsets

Actively transcribed genes have demethylated CpG islands, and the GC box is occupied by the transcription factor Sp1 (31, 32). To determine the binding of Sp1 to this enhancer, ChIP analyses were performed. In nTreg and Aza plus TGFβ Treg this CpG site was occupied by Sp1, but not in naive $CD4^+CD25^-$ T cells, activated $CD4^+$ T cells, or TGFβ-induced Treg (Fig. 4*A*). The specificity of binding of Sp1 to the sequence was confirmed by EMSA (Fig. 4*B*). This suggests that Sp1 binds the upstream Foxp3 enhancer and is involved in the function of the upstream *Foxp3* enhancer. Histone acetylation is an additional feature of chromatin remodeling and transcriptional activation (24, 33). ChIP assays for acetylated histone 3 (AcH3) showed that the upstream Foxp3 enhancer was acetylated in nTreg (>4.5-fold) and Aza plus TGFβ induced Treg (~3-fold), but not in activated $CD4^+$ T cells (~1.5-fold) or TGFβ-induced Treg (~1.1-fold) (Fig. 4*C*). Analysis predicted that upstream *Foxp3* enhancer possesses numerous TIEG1, EGR1, and AP-2a binding sites. TIEG1 and EGR1 are homologous and transcribed from differentially regulated, alternative promoters but use common exons in most all of their coding regions (34). Recently it has been shown that TIEG1 plays role in the Foxp3 expression and Treg function (35). ChIP analysis for TIEG1 showed significant binding to the upstream Foxp3 enhancer in Aza plus TGFβ induced Treg and nTreg compared with naive $CD4^+CD25^-$ T cells, activated T cells, or TGFβ-induced Treg (Fig. 4*D*). In contrast, AP-2a and EGR1 were not differentially bound in these subsets (supplemental Fig. S3, *B* and *C*).

To show that the upstream *Foxp3* enhancer is unique in its regulation, we also analyzed the Foxp3 proximal promoter located at the transcriptional start site (36). There was no significant difference in histone acetylation at this site between TGFβ or Aza plus TGFβ Treg (Fig. 4*C*), whereas nTreg had increased acetylation at this site (10-fold). Likewise, by ChIP assay there was no significant difference in pSmad2/3 binding between TGFβ-induced or Aza plus TGFβ-induced Treg at the Smad consensus site (Fig. 4*E*), although nTreg had increased binding (~8-fold). The role of TGFβ signaling was confirmed in $Smad3^{-/-}$ cells, where TGFβ-induced but not Aza-induced Foxp3 expression was inhibited compared with $Smad3^{+/+}$ controls (Fig. 4*F*). Importantly, the generation of thymic-derived nTreg is not affected in $TGF\beta1^{-/-}$ or $Smad3^{-/-}$ mice (37). Thus, the Foxp3 proximal promoter structure and responsiveness to TGFβ differs between nTreg and other Treg subsets, whereas the upstream Foxp3 enhancer is similar only between nTreg and Aza-induced Treg, suggesting that the upstream enhancer activity is specifically involved in nTreg but not in TGFβ-induced peripheral Treg generation and function.

IL-6 decreases Foxp3 expression and increases upstream Foxp3 enhancer CpG methylation in nTreg

IL-6 regulates the reciprocal development of Treg and Th17 (38) and inhibits Foxp3 expression and suppressive function in nTreg (39, 40). To determine whether the IL-6-induced loss of Foxp3 is due to changes in the upstream Foxp3 enhancer structure and transcription, highly purified $CD4^+CD25^+$ T cells were purified using flow cytometry (Fig. 5*A*). Purified nTreg were cultured with or without IL-6 and results showed that IL-6 inhibited both Foxp3 protein (Fig. 5*A*) and mRNA expression in nTreg (Fig. 5*B*). To confirm that the increase in $Foxp3^-CD4^+$ T cells was not due to overgrowth of $Foxp3^-$ T cells present at the initiation of culture, $CD4^+Foxp3gfp^+$ nTreg (90%) (CD45.2) were stimulated along with congenically marked naive $CD4^+CD25^-CD45.1^+$ cells (10%) in the presence or absence of IL-6 for 4 days. IL-6 down-regulated Foxp3gfp in $CD4^+CD45.1^-$ nTreg (supplemental Fig. S4), whereas the total percentage of $CD4^+CD45.1^+$ cells did not change significantly (IL-2, anti-CD3ε: 11.5%; IL-2, anti-CD3ε, TGFβ: 12.9%; IL-2, anti-CD3ε, TGFβ, IL-6: 8.61%), showing that the IL-6-induced increase in $Foxp3^-$ cells is not due to overgrowth of $CD4^+Foxp3^-$ T cells. ChIP analysis showed IL-6-induced deacetylation of histone 3 at the upstream *Foxp3* enhancer (Fig. 5*C*). To examine IL-6-induced inhibition in Foxp3 expression, $Foxp3gfp^+$ nTreg were purified from Foxp3gfp reporter mice. These purified $CD4^+Foxp3gfp^+$ nTreg cultured with IL-6 and TGFβ, and ~20% of the cells down-regulated Foxp3gfp expression. Analyses of purified subsets showed increased DNMT1 binding (Fig. 5*D*) and methylation of the upstream *Foxp3* enhancer (Fig. 5, *E* and *F*) and repression of *Foxp3* transcription (Fig. 5*G*) in $Foxp3gfp^-$ cells compared with $Foxp3gfp^+$ CD4 T cells. In the same cultures we did not observe IL-17 mRNA expression in the $Foxp3gfp^-$ or $Foxp3gfp^+$ T cells (data not shown). Importantly, IL-6 did not inhibit *Foxp3* expression in STAT3-deficient nTreg (Fig. 5*H*), showing that IL-6-induced CpG methylation and inhibition of Foxp3 expression are STAT3 dependent.

Characterization of Foxp3 induction and maintenance by Aza

Because DNMT inhibition by Aza is most effective in actively proliferating cells (41, 42), the timing of Aza exposure was examined. The results showed that 24 h of exposure starting at culture initiation, but not later times, was required to induce maximal Foxp3 expression (Fig. 6*A*, and data not shown). Thus, DNMT

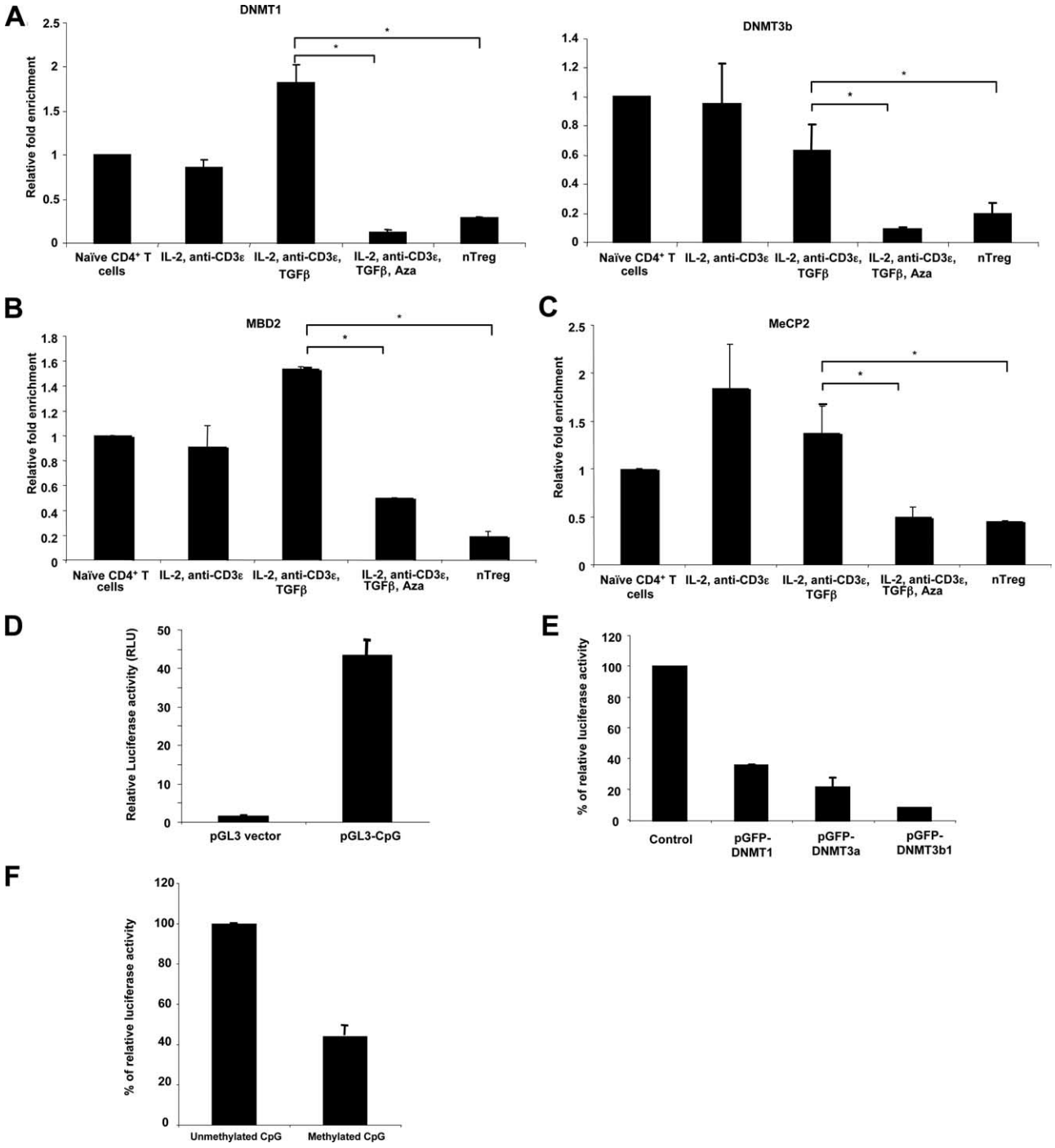

FIGURE 3. Foxp3 enhancer is occupied by DNMTs. $CD4^+CD25^-Foxp3gfp^-$ (naive) or $CD4^+CD25^+Foxp3gfp^+$ (nTreg) cells were purified from Foxp3gfp reporter male mice by flow cytometry. $CD4^+CD25^-Foxp3gfp^-$ T cells (50,000 cells/well) were cultured with irradiated, syngenic, T cell-depleted splenocytes (50,000 cells/well) along with anti-CD3ε mAb (1 μg/ml), IL-2 (10 ng/ml), TGFβ (5 ng/ml), and Aza (1 μM) for 4 days. Aza was removed after 24 h. After culture, $CD4^+CD25^+Foxp3gfp^+$ T cells were purified using flow cytometry. *A*, ChIP assay on upstream *Foxp3* enhancer using the indicated cells with anti-DNMT1 (*left*) and anti-DNMT3b (*right*). *B*, ChIP assay on upstream enhancer with anti-MBD2. *C*, ChIP assay on upstream enhancer with anti-MeCP2. *D*, BW5147.3 lymphoma T cells transfected with control vector (pGL3) or Foxp3 enhancer containing plasmid (pGL3-CpG). Luciferase activity was monitored 48 h after transfection. *E*, pGL3-CpG construct (3 μg) was cotransfected along with control plasmid, pGFP-DNMT1, pGFP-DNMT3a, or pGFP-DNMT3b1 (12 μg). Luciferase activity was monitored 48 h after transfection. *F*, Inhibition of enhancer activity by in vitro methylation of the upstream Foxp3 CpG enhancer site. Data were normalized to luciferase activity of control sample. Data shown are representative of 2–3 independent experiments for each panel. *, $p < 0.05$.

inhibition was required early and briefly during the initial proliferative cycle. Monitoring expression with respect to proliferation (CFSE dilution) showed that Foxp3 was expressed early after the initial division in TGFβ Treg and Aza plus TGFβ Treg, and Foxp3 did not increase or accumulate with more division cycles (Fig. 6*B*). A gene dosage effect was not observed in male compared with female cells (data not shown). Apoptosis, proliferation, and cell accumulation were not significantly different in ZyCyd plus TGFβ-induced Treg compared with TGFβ-induced Treg (supplemental Fig. S5*A*). To measure the stability of expression, Treg

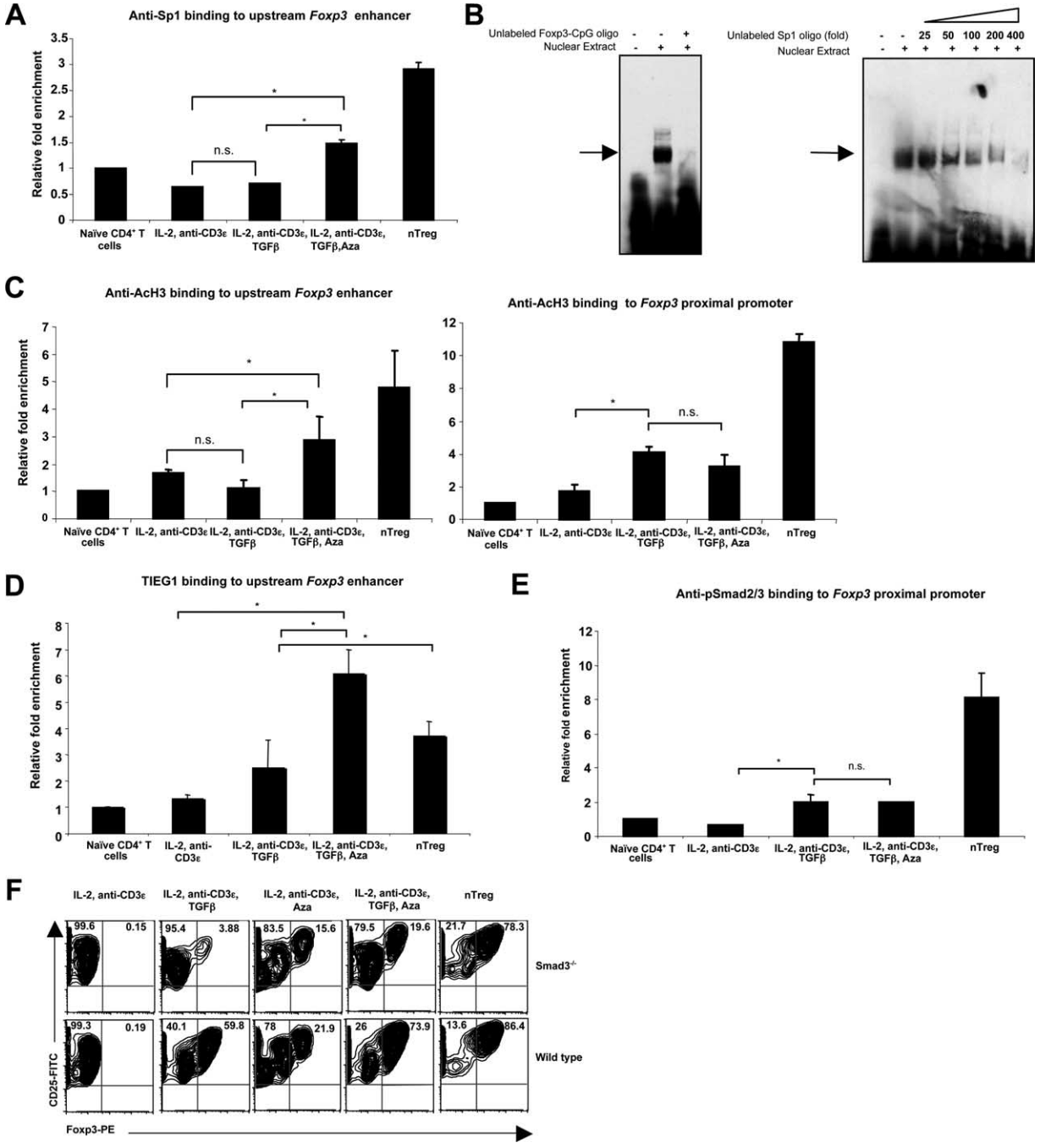

FIGURE 4. Foxp3 upstream enhancer of Aza plus TGFβ Treg is transcriptionally active. $CD4^+CD25^-Foxp3gfp^-$ (naive) or $CD4^+CD25^+Foxp3gfp^+$ (nTreg) cells were purified from Foxp3gfp reporter male mice by flow cytometry. $CD4^+CD25^-Foxp3gfp^-$ T cells (50,000 cells/well) were cultured with irradiated, syngenic, T cell-depleted splenocytes (50,000 cells/well) along with anti-CD3ε mAb (1 μg/ml), IL-2 (10 ng/ml), TGFβ (5 ng/ml), and Aza (1 μM) for 4 days. Aza was removed after 24 h. After culture, $CD4^+CD25^+Foxp3gfp^+$ T cells were purified again using flow cytometry. *A*, ChIP assay for upstream *Foxp3* enhancer using the indicated cells and anti-mouse Sp1. *B*, EMSA with *Foxp3* enhancer CpG oligonucleotide (20 fmol), Aza plus TGFβ-induced Treg nuclear extract (10 μg), and 200-fold excess unlabeled *Foxp3* enhancer CpG oligonucleotide. Competition EMSA with *Foxp3* enhancer CpG oligonucleotide, Aza plus TGFβ-induced Treg nuclear extract, and graded amounts of unlabeled Sp1 consensus oligonucleotide. *C*, TGFβ or Aza plus TGFβ-induced $CD4^+CD25^+Foxp3gfp^+$ Treg were generated by culturing $CD4^+CD25^-Foxp3gfp^-$ T cells as described in *A*. ChIP assay was conducted for AcH3 binding to the upstream Foxp3 enhancer (*left*) and the proximal promoter (*right*). *D*, ChIP assay for TIEG1 at upstream Foxp3 enhancer was performed from the cultured cells described above. *E*, ChIP assay for pSmad2/3 at *Foxp3* proximal promoter was performed from the cultured cells described above. *F*, $CD4^+CD25^-$ T cells were purified from $Smad3^{-/-}$ or wild-type male mice spleen using flow cytometry. Foxp3 expression in $Smad3^{-/-}$ and wild-type T cells after 4 days of culture (Aza at 1 μM for 24 h). Intracellular Foxp3 expression was analyzed by gating on $CD4^+$ cells. Data are representative of 2–3 independent experiments. $*$, $p < 0.05$; n.s., not significant.

were generated, purified, and recultured. The Aza plus TGFβ-induced Treg maintained a much higher percentage of $Foxp3^+$ cells compared with TGFβ-induced Treg (Fig. 6*C*).

Activated T cells that have undergone other differentiation pathways do not usually differentiate toward the $Foxp3^+$ Treg fate (43). Because Aza might reprogram cells by altering gene methylation, we

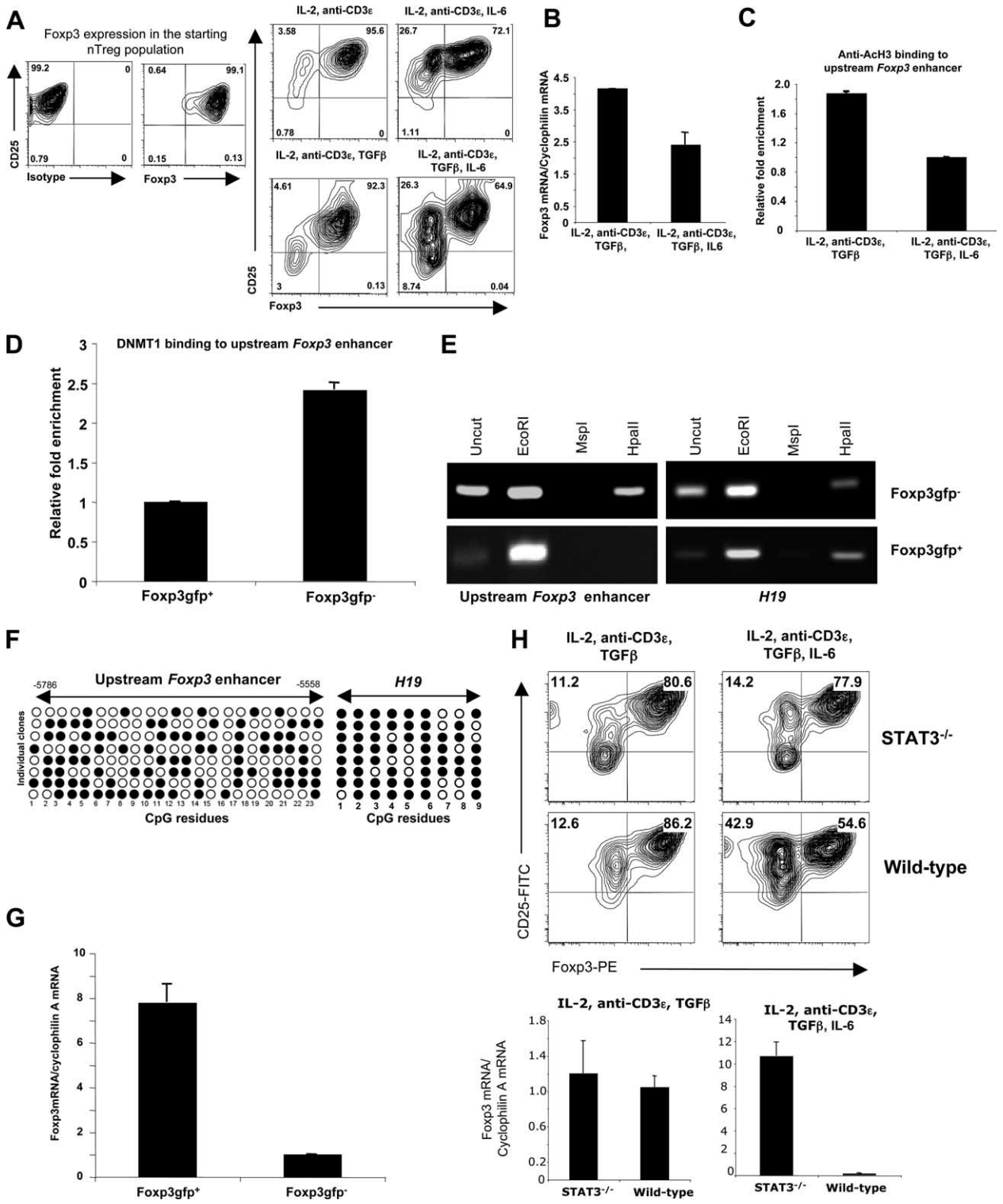

FIGURE 5. IL-6 down-regulates Foxp3 expression in nTreg. *A*, $CD4^+CD25^+$ T cells were purified from the BALB/c male mouse spleens by flow cytometry. Freshly isolated $CD4^+CD25^+$ T cells (5×10^4 cells/well) from BALB/c mice were cultured with IL-2, anti-CD3ε mAb, and TGFβ with or without IL-6 (20 ng/ml) and APC for 4 days. Intracellular Foxp3 expression was monitored by gating on $CD4^+$ cells. *B*, *Foxp3* mRNA expression from the above cultures was analyzed by qRT-PCR. *C*, $CD4^+$ T cells from the above cultures were subjected to ChIP assay for AcH3 at the upstream Foxp3 enhancer. *D*, Freshly purified $CD4^+Foxp3gfp^+$ T cells (5×10^4 cells/well) from Foxp3gfp male mice were cultured with IL-2, anti-CD3ε mAb, TGFβ, IL-6, and APC for 6 days and separate $Foxp3gfp^+$ and $Foxp3gfp^-$ CD4 T cells were then purified using flow cytometry. DNMT1 binding on the upstream *Foxp3* enhancer was analyzed by ChIP assay. *E*, Methyl-specific restriction digestion of genomic DNA of upstream *Foxp3* enhancer and *H19* promoters. *F*, Disulfite sequencing of the upstream *Foxp3* enhancer and *H19* in TGFβ plus IL-6 induced $Foxp3gfp^-$ nTreg. The methylation pattern of each clone obtained is shown. ●, Methylated CpG; ○, nonmethylated CpG. *G*, qRT-PCR analysis of *Foxp3* mRNA. *H*, $CD4^+CD25^+$ T cells (5×10^4 cells/well) were purified from the $STAT3^{-/-}$ (CD4 Cre:STAT3 f/f) or littermate control male mice and cultured with IL-2, anti-CD3ε mAb, TGFβ, IL-6, and APC for 4 days. Intracellular Foxp3 expression was analyzed by gating on $CD4^+$ cells (*top*). *Foxp3* mRNA expression was analyzed by qRT-PCR from the same cells (*bottom*). Data are representative two independent experiments for entire figure.

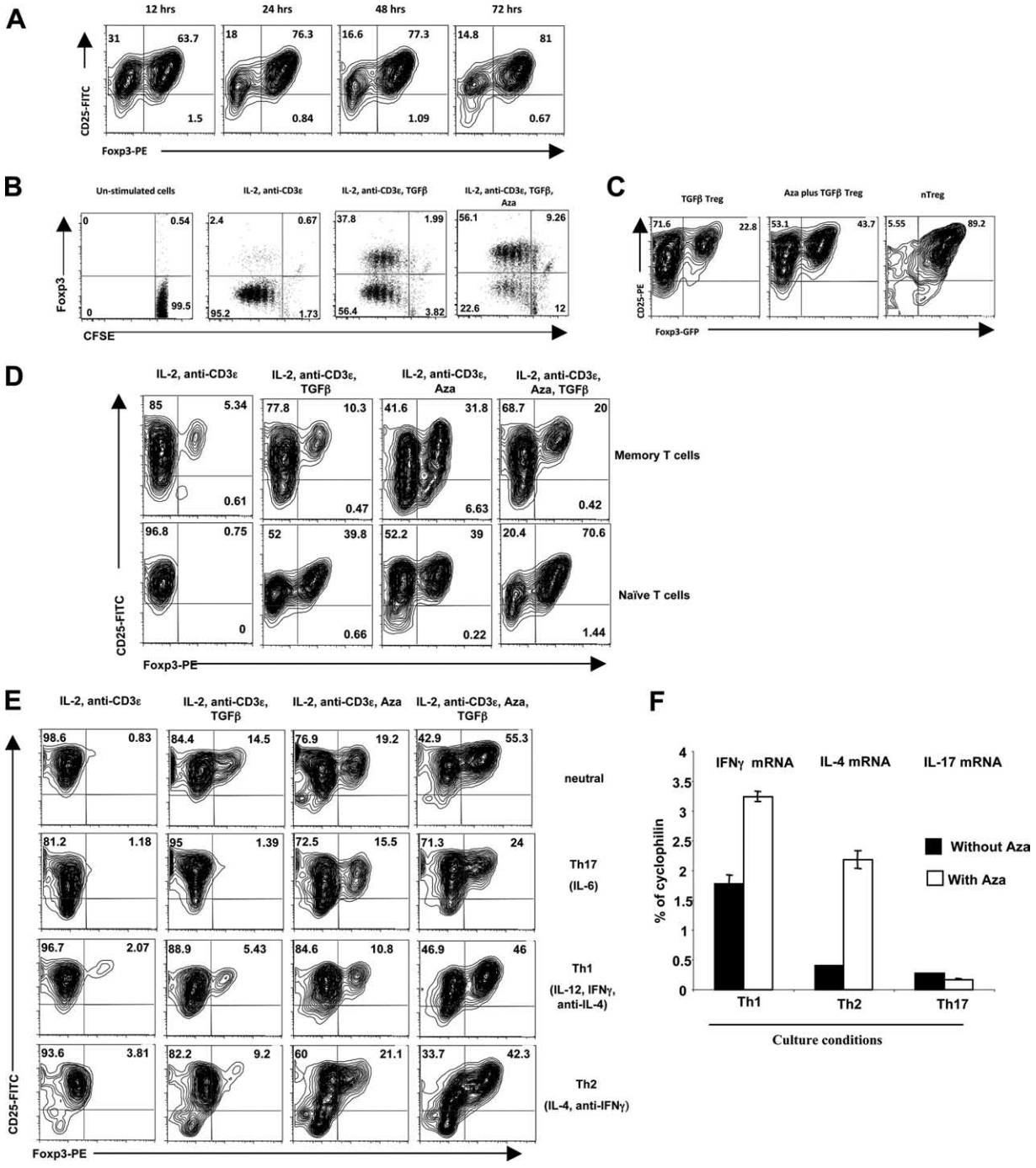

FIGURE 6. Induction of Foxp3 in T cell subsets. *A*, $CD4^+CD25^-$ T cells were purified from BALB/c male spleens using flow cytometry. $CD4^+CD25^-$ T cells were cultured with APC, IL-2, anti-CD3ε mAb, Aza (1.25 μM), and TGFβ (5 ng/ml). Aza was removed from the culture at the indicated time points and the cells were recultured for up to a total of 4 days. Intracellular Foxp3 expression was analyzed by gating on $CD4^+$ cells. *B*, CFSE labeled-$CD4^+CD25^-$ T cells cultured in the indicated conditions for 4 days (Aza at 1.25 μM for 24 h) and intracellular Foxp3 and CFSE dilution analyzed by gating on $CD4^+$ cells. *C*, $CD4^+CD25^-Foxp3gfp^-$ T cells (naive) and $CD4^+CD25^+Foxp3gfp^+$ T cells (nTreg) were purified from the Foxp3gfp reporter male spleens using flow cytometry. TGFβ or Aza plus TGFβ-induced $CD4^+CD25^+Foxp3gfp^+$ Tregs were generated by a 4-day culture of $CD4^+CD25^-Foxp3gfp^-$ T cells. $CD4^+CD25^+Foxp3gfp^+$ Tregs were purified from the indicated cultures and then recultured in the presence of IL-2, anti-CD3ε mAb, and APC for an additional 4 days. Stability of Foxp3gfp expression was analyzed by gating on $CD4^+$ cells. *D*, $CD4^+CD25^-CD62L^{high}CD44^{low}$ (naive) and $CD4^+CD25^-CD62L^{low}CD44^{high}$ (memory) cells were isolated from BALB/c male spleens by flow cytometric sorting and cultured. Foxp3 expression was analyzed by gating on $CD4^+$ cells. *E*, $CD4^+CD25^-$ T cells were purified from BALB/c male spleens using flow cytometry. $CD4^+CD25^-$ T cells were cultured with APC, anti-CD3ε mAb, IL-2, Aza (1 μM for 24 h), and the indicated mAb and cytokines for 5 days. Th1 conditions were IL-12 (5 ng/ml), IFN-γ (20 ng/ml), and anti-IL-4 mAb (10 μg/ml), Th2 conditions were IL-4 (10 ng/ml) and anti-IFN-γ (10 μg/ml), and Th17 conditions were IL-6 (10 ng/ml) and TGFβ (5 ng/ml). Foxp3 expression was analyzed by gating on $CD4^+$ cells. *F*, Cytokine mRNA expression from cells cultured with anti-CD3ε mAb, IL-2, APC, and the indicated Th culture conditions with or without Aza (1 μM for 24 h). Data are representative of 2–4 independent experiments.

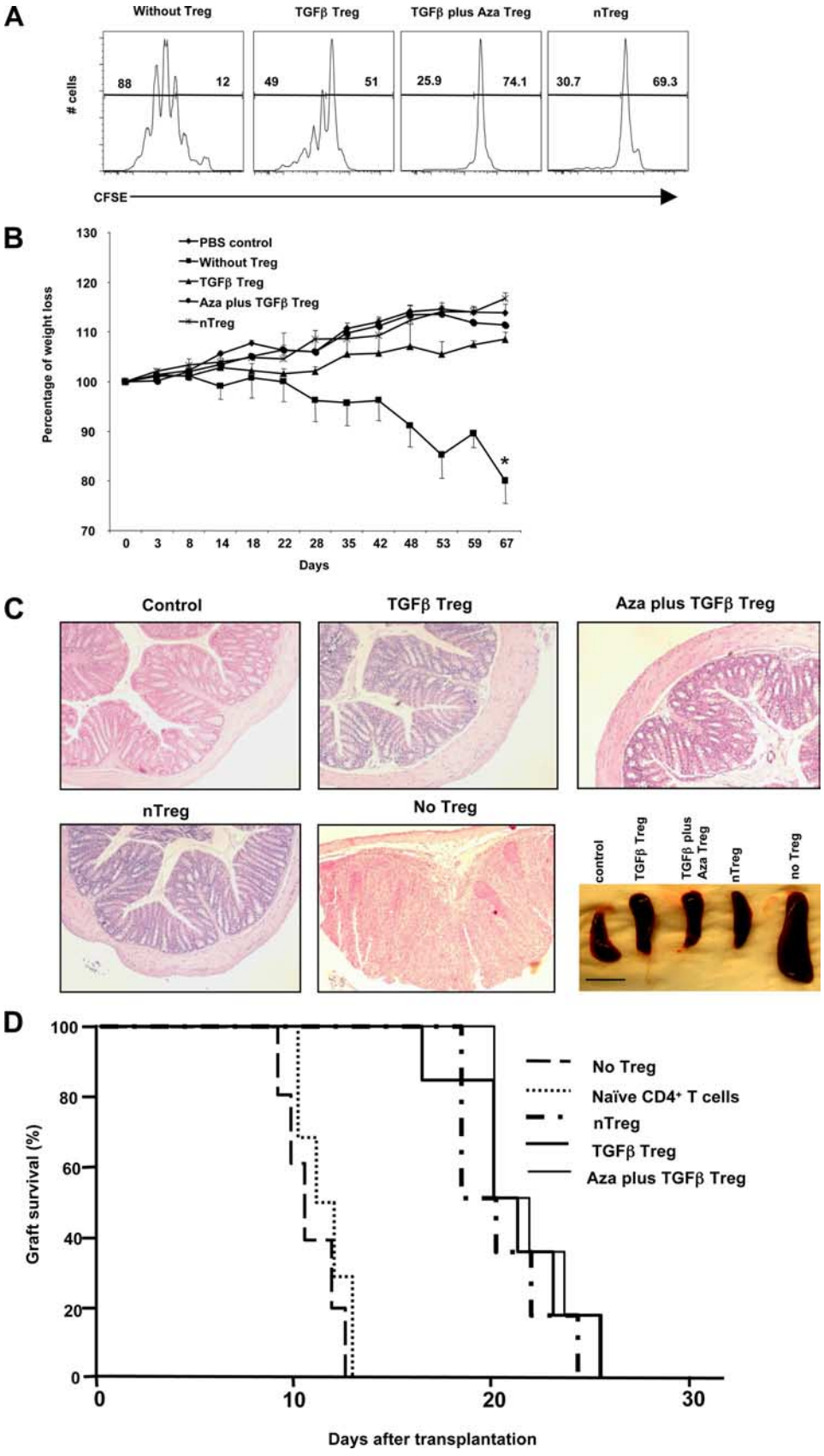

FIGURE 7. Aza plus TGFβ Treg are suppressive. *A*, Freshly isolated $CD4^+CD25^-$ T cells from BALB/c male were sorted and labeled with CFSE and 5×10^4 cells per well were cultured with the indicated Treg subsets (5×10^4 cells/well) in the presence of APC and anti-CD3ε mAb (1 μg/ml) for 72 h. Proliferation of T cells was measured by CFSE dilution. Percentages of divided and undivided cells are shown. *B*, Aza plus TGFβ Treg prevent autoimmune colitis. *C*, B-17 SCID mice were injected i.p. with $CD4^+CD25^-CD45RB^{high}$ T cells (5×10^5) purified from BALB/c mice either alone or together with purified, cultured $CD4^+CD25^+Foxp3gfp^+$ Treg subsets as indicated (2.5×10^5 cells/mouse). Weights were measured at the indicated times; $n = 4$–5 mice/group. *C*, Histopathology of the colon and spleen sizes 67 days after T cell reconstitution. Original magnification was ×100. Scale bar, 1 cm. *D*, Streptozotocin-induced diabetic BALB/c mice received C57BL/6 mice islets (400 islets/mouse) underneath the right kidney capsule along with purified cultured $CD4^+CD25^+Foxp3gfp^+$ Treg (1×10^6 cells/mouse) injected i.v. Blood glucose levels were monitored daily; $n = 6$ mice/group ($p < 0.001$ for all subsets of Treg vs no Treg or naive $CD4^+$ T cell group; $p > 0.05$ for Aza plus TGFβ Treg vs TGFβ Treg or nTreg). Data are representative of 2–5 independent experiments.

determined whether previously activated cells could be induced to express Foxp3. $CD4^+CD25^-$ T cells were stimulated, rested, and then restimulated with Aza. Preactivated T cells could not be induced to express Foxp3 (supplemental Fig. S5*B*), although they were very sensitive to the antiproliferative effect of Aza treatment (data not shown). Other time intervals for primary stimulation followed by restimulation with Aza did not induce Foxp3 expression (data not shown). Further analysis showed that Aza could not induce strong

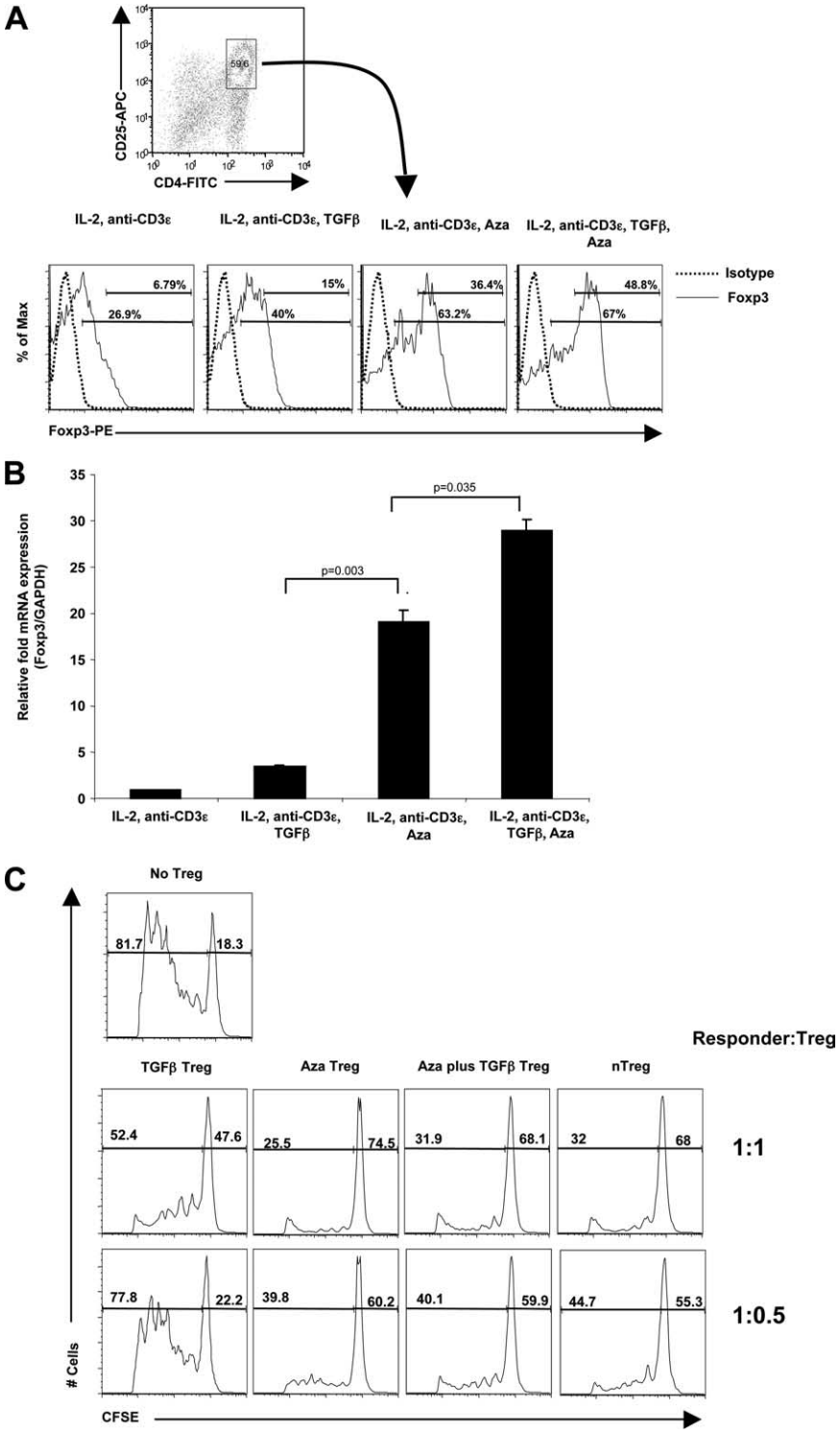

FIGURE 8. Aza plus TGFβ induce Foxp3 expression and suppressive function in human $CD4^+CD25^-$ T cells. *A*, $CD4^+CD25^-$ T cells (5×10^4 cells/well) purified from PBMC were cultured with syngeneic $CD4^+$ T cell-depleted PBMC (5×10^4 cells/well) with anti-CD3ε mAb, IL-2 (10 ng/ml), TGFβ (5 ng/ml) or Aza (1 μM) for 6 days. Aza was removed after 24 h. Intracellular Foxp3 expression was monitored by flow cytometry. Data are representative of three independent experiments with different blood donors. *B*, Foxp3 mRNA expression from cells in *A*. *C*, Freshly purified, CFSE-labeled $CD4^+CD25^-$ T cells were cultured with different ratios of purified cultured $CD4^+CD25^+$ Treg subsets along with irradiated T cell-depleted autologous PBMCs and anti-human CD3ε mAb for 96 h. Data are representative of three independent experiments.

Foxp3 expression in $CD4^+CD44^{high}CD62L^{low}$ (memory) T cells in combination with TGFβ but did so in $CD4^+CD44^{low}CD62L^{high}$ (naive) T cells (Fig. 6*D*), suggesting that apart from CpG demethylation, there were other dominant pathways and factors that played essential roles in Foxp3 expression. To determine whether other signals influenced Aza and TGFβ-driven Treg differentiation or whether Aza influenced T cell differentiation to other lineages, cultures were established that incorporated Aza and other Th conditions. The results showed that IL-6 along with TGFβ (Th17 conditions) inhibited Foxp3 expression, whereas Th1 and Th2 cytokines had only minor effects on Foxp3 expression in combination with TGFβ and Aza (Fig. 6*E*). Th1, Th2, and Th17 cytokines were measured in their cognate culture conditions. Aza increased the expression of IFN-γ in Th1 and IL-4 in Th2 cultures, but not IL-17 in Th17 cultures (Fig. 6*F*). Together, the results suggested that DNMT inhibition is most effective at driving T cells into the Treg lineage (Fig. 6*E*), but that this strategy may be used to drive some but not all other lineages.

Aza plus TGFβ-induced Treg are suppressive

Because Aza plus TGFβ-induced Treg resembled conventional nTreg (supplemental Fig. S2, *D* and *E*), their functional activities

were evaluated. Aza plus TGFβ-induced Treg inhibited proliferation of $CD4^+CD25^-$ T cells (Fig. 7*A*) and were similar in potency to nTreg. Aza plus TGFβ-induced Treg inhibited $CD4^+CD25^-$ $CD45RB^{high}$ T cell-induced colitis and splenomegaly in CB17. SCID (Fig. 7, *B* and *C*), and recipients sustained ~2-fold more splenic $Foxp3^+$ T cells over time compared with mice that received TGFβ-induced Treg (supplemental Fig. S6). Adoptive transfer of Aza plus TGFβ-induced Treg also prolonged pancreatic islet allograft survival (Fig. 7*D*). Together, the results demonstrated potent and stable suppressor function.

Aza plus TGFβ induce suppressive $Foxp3^+CD4^+$ human T cells

$CD4^+CD25^-$ T cells were isolated from human PBMC and cultured in the presence of IL-2, anti-CD3ε mAb, TGFβ, and Aza for 6 days. Aza plus TGFβ induced a higher percentage of $Foxp3^+$ cells (67%) (Fig. 8*A*), a greater number of Foxp3 bright cells (48.8%), and enhanced *Foxp3* gene expression compared with TGFβ alone (36.4%) (Fig. 8*B*). Foxp3 is an activation marker but not an exclusive Treg marker in man, so human TGFβ-induced Treg are not necessarily anergic or suppressive (44). To determine whether Aza also induced regulatory function, a suppression assay was performed. Aza plus TGFβ-induced Treg were almost as suppressive as $CD4^+CD25^+$ nTreg, whereas TGFβ-induced Treg had less suppressive potency, particularly at higher cell ratios (Fig. 8*C*). This suggested that low Foxp3 expression in IL-2 plus anti-CD3ε mAb or IL-2 plus anti-CD3ε mAb plus TGFβ-stimulated human T cells were not sufficient for conversion to functional suppressive Treg activity (Fig. 8, *A* and *B*).

Discussion

This study demonstrated differential *Foxp3* gene regulation and structure in nTreg compared with TGFβ-induced Treg or other naive or activated $CD4^+$ T cells. There is a unique and highly conserved upstream CpG-rich enhancer in the *Foxp3* gene that was demethylated and highly active in nTreg but methylated in TGFβ-induced peripheral Treg. Sp1, AcH3, TIEG1, MeCP2, MBD2, DNMT1, and DNMT3b were central elements for its function and structure and were differentially bound to this site in nTreg compared with TGFβ-induced Treg. Importantly, the use of a DNMT inhibitor demethylated and activated the upstream *Foxp3* enhancer to induce Foxp3 expression and subsequently allowed the induction of Foxp3-dependent, Treg-restricted sets of genes. Demethylation acted synergistically with TGFβ to convert a variety of naive T cells to Treg with high Foxp3 expression and potent, stable suppressive function. Conversely, IL-6 induced methylation of the upstream *Foxp3* enhancer and repression of *Foxp3* expression.

Some structural and development differences between nTreg and TGFβ-induced peripheral Treg have been shown in other analyses (7, 16, 19). TGFβ partially down-regulates CpG methylation of the Foxp3 proximal promoter and an intronic enhancer so that TCR-induced CREB/ATF bind to the demethylated intronic enhancer (7), suggesting a role in TGFβ Treg. However, nTreg had greater transcriptional activity and demethylation compared with TGFβ-induced Treg (7, 16) suggesting other as yet undefined regulatory signals. A second non-CpG intronic enhancer region is responsive to NFAT and Smad3 in both nTreg and TGFβ Treg (19), suggesting a role for TCR or perhaps other signals. $Smad3^{-/-}$, dominant negative TGFβ receptor II, or $TGF\beta1^{-/-}$ mice do not have defects in the development of thymic-derived nTreg (37, 45, 46), suggesting that TGFβ is involved only in peripheral Treg generation. However, a recent report demonstrated a critical role for TGFβ receptor I, yet this requirement could be bypassed by IL-2/IL-2R signaling (47). Our data demonstrated additional differences between these Treg subsets at the proximal promoter near the transcriptional start site so that nTreg had greater TGFβ-regulated Smad2/3 signaling and histone 3 acetylation. This latter finding is consistent with the recent report that inhibition of HDAC induces Foxp3 expression in T cells (48). However, studies using specific genetic knockouts of *Foxp3* intronic or upstream enhancers will provide more insight about the regulation of *Foxp3* transcription and Treg function.

Our data demonstrated an important upstream *Foxp3* enhancer ~5 kb upstream of the transcriptional start site. This element was differentially methylated and active, comparing nTreg and TGFβ-induced peripheral Treg. In contrast to the proximal promoter and intronic enhancer, TGFβ did not regulate its structure or function. Aza demethylated this element, inducing gene expression and a cellular phenotype that closely resembled that of nTreg. In a different system, Aza induced Foxp3 in human NK cells through an IL-2/IL-2R/STAT5-dependent mechanism (49), as well as demethylating the intronic Foxp3 enhancer (18), supporting our findings that Aza acted independently of TGFβ signaling. IL-2/IL-2R/STAT5 signaling is required for Treg development and *Foxp3* expression (8), although their precise effects on gene structure and transcription are not currently known. There are 11 STAT5 binding sites predicted close to the *Foxp3* proximal promoter, and three sites highly conserved in mammals are transcriptionally active (8). It has been reported that Th1/Th2-polarized T cells do not express Foxp3 after stimulation with TGFβ (50, 51), but in the current study we show that culturing such cells in the presence of Aza can induce Foxp3 expression. Together, these findings suggest that, like the Th1 and Th2 loci (20), there is a Treg locus with several regions, epigenetically regulated and involved in the development of nTreg (supplemental Fig. S7).

Activated T cells express high levels of STAT3 that induce the transcription of DNMT1 (52), and high levels of DNMT1 may repress Foxp3 expression in preactivated or differentiated T cells (53). It is noteworthy that IL-6 signals via STAT3, resulting in methylation of the upstream *Foxp3* enhancer and repression of *Foxp3* expression. Our results demonstrated that TGFβ did not induce Foxp3 in resting memory $CD4^+$ T cells, whereas Aza induced only low-level Foxp3 expression. Inhibition of DNMTs in preactivated $CD4^+$ T cells also did not induce Foxp3. This suggests that other dominant factors were essential for *Foxp3* transcription so that DNMT inhibitors do not lead to T cell reprogramming of previously differentiated T cells. Results with Th1, Th2, and Th17 culture conditions showed that DNMT inhibition potentiated other T cell differentiative pathways, although the preferred effect favored Foxp3 expression and the Treg lineage. It is interesting to speculate that this class of drugs induces $Foxp3^+$ Treg during cancer therapy, perhaps synergizing with tumor-produced TGFβ, which is associated with failure of immunotherapy and with tumor progression (3). Our results also imply that IL-6 could inhibit or even reverse the development of such Treg.

Foxp3 expression in human $CD4^+$ T cells does not necessarily denote a regulatory phenotype (44, 54). Human T cells express two Foxp3 isoforms, and enhanced expression is required for regulatory effector function (55). The *Foxp3* regulatory elements are methylated in TGFβ-induced $CD4^+$T cells (17), which might lead to low Foxp3 expression that is insufficient to imprint the regulatory phenotype. We showed that Aza enhanced Foxp3 expression in human $CD4^+$ T cells and that Aza-induced Treg, but not TGFβ-induced Treg, were suppressive. Our data and that of others demonstrated that even in the murine system there are differences between nTreg and TGFβ-induced Treg in regulation of the *Foxp3*

expression and suppressor activity (7, 16). This suggests that nTreg are more potent and stable suppressors than TGFβ-induced Treg, and DNMT inhibition induces Treg that more closely resemble nTreg.

Induced Treg have the potential to be used in clinical treatments (1). Using both TCR transgenic and nontransgenic cells, we demonstrated that large numbers of Treg could be generated with Ag-specific stimulation. We also demonstrated that Aza plus TGFβ-induced Treg prevented autoimmune colitis and prolonged islet allograft survival. The techniques developed here are similar to protocols for adoptive transfer of leukocytes for bone marrow transplantation or immunotherapy. Further, our techniques used drugs and biologics such as IL-2, anti-CD3ε mAb, and DNMT inhibitors for which there are already substantial clinical experience and regulatory approval. The combination of DNMT and HDAC inhibitors may further boost nTreg development (48).

Acknowledgments

We thank Drs. Alexander Rudensky, Heinrich Leonhardt, Chuxia Deng, and En Li for providing valuable reagents. We also acknowledge the assistance of Minwie Mao, Dan Chen, and all the volunteers for their generous donation of blood.

Disclosures

The authors have no financial conflict of interest.

References

1. Sakaguchi, S., and F. Powrie. 2007. Emerging challenges in regulatory T cell function and biology. *Science* 317: 627–629.
2. van Maurik, A., M. Herber, K. J. Wood, and N. D. Jones. 2002. Cutting edge: $CD4^+CD25^+$ alloantigen-specific immunoregulatory cells that can prevent $CD8^+$ T cell-mediated graft rejection: implications for anti-CD154 immunotherapy. *J. Immunol.* 169: 5401–5404.
3. Wang, H. Y., and R. F. Wang. 2007. Regulatory T cells and cancer. *Curr. Opin. Immunol.* 19: 217–223.
4. Marie, J. C., J. J. Letterio, M. Gavin, and A. Y. Rudensky. 2005. TGF-β1 maintains suppressor function and Foxp3 expression in $CD4^+CD25^+$ regulatory T cells. *J. Exp. Med.* 201: 1061–1067.
5. Fontenot, J. D., J. P. Rasmussen, L. M. Williams, J. L. Dooley, A. G. Farr, and A. Y. Rudensky. 2005. Regulatory T cell lineage specification by the forkhead transcription factor foxp3. *Immunity* 22: 329–341.
6. Fontenot, J. D., J. P. Rasmussen, M. A. Gavin, and A. Y. Rudensky. 2005. A function for interleukin 2 in Foxp3-expressing regulatory T cells. *Nat. Immunol.* 6: 1142–1151.
7. Kim, H. P., and W. J. Leonard. 2007. CREB/ATF-dependent T cell receptor-induced FoxP3 gene expression: a role for DNA methylation. *J. Exp. Med.* 204: 1543–1551.
8. Burchill, M. A., J. Yang, C. Vogtenhuber, B. R. Blazar, and M. A. Farrar. 2007. IL-2 receptor β-dependent STAT5 activation is required for the development of $Foxp3^+$ regulatory T cells. *J. Immunol.* 178: 280–290.
9. Chen, W., W. Jin, N. Hardegen, K. J. Lei, L. Li, N. Marinos, G. McGrady, and S. M. Wahl. 2003. Conversion of peripheral $CD4^+CD25^-$ naive T cells to $CD4^+CD25^+$ regulatory T cells by TGF-β induction of transcription factor Foxp3. *J. Exp. Med.* 198: 1875–1886.
10. Fu, S., N. Zhang, A. C. Yopp, D. Chen, M. Mao, D. Chen, H. Zhang, Y. Ding, and J. S. Bromberg. 2004. TGF-β induces $Foxp3^+$ T-regulatory cells from $CD4^+$ $CD25^-$ precursors. *Am. J. Transplant.* 4: 1614–1627.
11. Fontenot, J. D., M. A. Gavin, and A. Y. Rudensky. 2003. Foxp3 programs the development and function of $CD4^+CD25^+$ regulatory T cells. *Nat. Immunol.* 4: 330–336.
12. Williams, L. M., and A. Y. Rudensky. 2007. Maintenance of the Foxp3-dependent developmental program in mature regulatory T cells requires continued expression of Foxp3. *Nat. Immunol.* 8: 277–284.
13. Bluestone, J. A. 2005. Regulatory T-cell therapy: is it ready for the clinic? *Nat. Rev.* 5: 343–349.
14. Ng, H. H., Y. Zhang, B. Hendrich, C. A. Johnson, B. M. Turner, H. Erdjument-Bromage, P. Tempst, D. Reinberg, and A. Bird. 1999. MBD2 is a transcriptional repressor belonging to the MeCP1 histone deacetylase complex. *Nat. Genet.* 23: 58–61.
15. Feng, Q., and Y. Zhang. 2001. The MeCP1 complex represses transcription through preferential binding, remodeling, and deacetylating methylated nucleosomes. *Genes Dev.* 15: 827–832.
16. Floess, S., J. Freyer, C. Siewert, U. Baron, S. Olek, J. Polansky, K. Schlawe, H. D. Chang, T. Bopp, E. Schmitt, et al. 2007. Epigenetic control of the foxp3 locus in regulatory T cells. *PLoS Biol.* 5: e38.
17. Baron, U., S. Floess, G. Wieczorek, K. Baumann, A. Grutzkau, J. Dong, A. Thiel, T. J. Boeld, P. Hoffmann, M. Edinger, et al. 2007. DNA demethylation in the human FOXP3 locus discriminates regulatory T cells from activated $FOXP3^+$ conventional T cells. *Eur. J. Immunol.* 37: 2378–2389.
18. Polansky, J. K., K. Kretschmer, J. Freyer, S. Floess, A. Garbe, U. Baron, S. Olek, A. Hamann, H. von Boehmer, and J. Huehn. 2008. DNA methylation controls Foxp3 gene expression. *Eur. J. Immunol.* 38: 1654–1663.
19. Tone, Y., K. Furuuchi, Y. Kojima, M. L. Tykocinski, M. I. Greene, and M. Tone. 2008. Smad3 and NFAT cooperate to induce Foxp3 expression through its enhancer. *Nat. Immunol.* 9: 194–202.
20. Lee, G. R., S. T. Kim, C. G. Spilianakis, P. E. Fields, and R. A. Flavell. 2006. T helper cell differentiation: regulation by cis elements and epigenetics. *Immunity* 24: 369–379.
21. Soutto, M., W. Zhou, and T. M. Aune. 2002. Cutting edge: distal regulatory elements are required to achieve selective expression of IFN-γ in Th1/Tc1 effector cells. *J. Immunol.* 169: 6664–6667.
22. Spilianakis, C. G., and R. A. Flavell. 2004. Long-range intrachromosomal interactions in the T helper type 2 cytokine locus. *Nat. Immunol.* 5: 1017–1027.
23. Ansel, K. M., D. U. Lee, and A. Rao. 2003. An epigenetic view of helper T cell differentiation. *Nat. Immunol.* 4: 616–623.
24. Agarwal, S., and A. Rao. 1998. Modulation of chromatin structure regulates cytokine gene expression during T cell differentiation. *Immunity* 9: 765–775.
25. Fields, P. E., G. R. Lee, S. T. Kim, V. V. Bartsevich, and R. A. Flavell. 2004. Th2-specific chromatin remodeling and enhancer activity in the Th2 cytokine locus control region. *Immunity* 21: 865–876.
26. Yang, X., J. J. Letterio, R. J. Lechleider, L. Chen, R. Hayman, H. Gu, A. B. Roberts, and C. Deng. 1999. Targeted disruption of SMAD3 results in impaired mucosal immunity and diminished T cell responsiveness to TGF-β. *EMBO J.* 18: 1280–1291.
27. Gimeno, R., C. K. Lee, C. Schindler, and D. E. Levy. 2005. Stat1 and Stat2 but not Stat3 arbitrate contradictory growth signals elicited by α/β interferon in T lymphocytes. *Mol. Cell. Biol.* 25: 5456–5465.
28. Kersh, E. N., D. R. Fitzpatrick, K. Murali-Krishna, J. Shires, S. H. Speck, J. M. Boss, and R. Ahmed. 2006. Rapid demethylation of the IFN-γ gene occurs in memory but not naive CD8 T cells. *J. Immunol.* 176: 4083–4093.
29. Kantarjian, H. M., S. O'Brien, J. Cortes, F. J. Giles, S. Faderl, J. P. Issa, G. Garcia-Manero, M. B. Rios, J. Shan, M. Andreeff, et al. 2003. Results of decitabine (5-aza-2′deoxycytidine) therapy in 130 patients with chronic myelogenous leukemia. *Cancer* 98: 522–528.
30. Fujimura, S., T. Matsui, K. Kuwahara, K. Maeda, and N. Sakaguchi. 2008. Germinal center B-cell-associated DNA hypomethylation at transcriptional regions of the AID gene. *Mol. Immunol.* 45: 1712–1719.
31. Brandeis, M., D. Frank, I. Keshet, Z. Siegfried, M. Mendelsohn, A. Nemes, V. Temper, A. Razin, and H. Cedar. 1994. Sp1 elements protect a CpG island from de novo methylation. *Nature* 371: 435–438.
32. Macleod, D., J. Charlton, J. Mullins, and A. P. Bird. 1994. Sp1 sites in the mouse aprt gene promoter are required to prevent methylation of the CpG island. *Genes Dev.* 8: 2282–2292.
33. Narlikar, G. J., H. Y. Fan, and R. E. Kingston. 2002. Cooperation between complexes that regulate chromatin structure and transcription. *Cell* 108: 475–487.
34. Subramaniam, M., J. R. Hawse, S. A. Johnsen, and T. C. Spelsberg. 2007. Role of TIEG1 in biological processes and disease states. *J. Cell. Biochem.* 102: 539–548.
35. Venuprasad, K., H. Huang, Y. Harada, C. Elly, M. Subramaniam, T. Spelsberg, J. Su, and Y. C. Liu. 2008. The E3 ubiquitin ligase Itch regulates expression of transcription factor Foxp3 and airway inflammation by enhancing the function of transcription factor TIEG1. *Nat. Immunol.* 9: 245–253.
36. Mantel, P. Y., N. Ouaked, B. Ruckert, C. Karagiannidis, R. Welz, K. Blaser, and C. B. Schmidt-Weber. 2006. Molecular mechanisms underlying FOXP3 induction in human T cells. *J. Immunol.* 176: 3593–3602.
37. Kullberg, M. C., V. Hay, A. W. Cheever, M. Mamura, A. Sher, J. J. Letterio, E. M. Shevach, and C. A. Piccirillo. 2005. TGF-β1 production by $CD4^+$ $CD25^+$ regulatory T cells is not essential for suppression of intestinal inflammation. *Eur. J. Immunol.* 35: 2886–2895.
38. Bettelli, E., Y. Carrier, W. Gao, T. Korn, T. B. Strom, M. Oukka, H. L. Weiner, and V. K. Kuchroo. 2006. Reciprocal developmental pathways for the generation of pathogenic effector TH17 and regulatory T cells. *Nature* 441: 235–238.
39. Doganci, A., T. Eigenbrod, N. Krug, G. T. De Sanctis, M. Hausding, V. J. Erpenbeck, B. el Haddad, H. A. Lehr, E. Schmitt, T. Bopp, et al. 2005. The IL-6R α chain controls lung $CD4^+CD25^+$ Treg development and function during allergic airway inflammation in vivo. *J. Clin. Invest.* 115: 313–325.
40. Pasare, C., and R. Medzhitov. 2003. Toll pathway-dependent blockade of $CD4^+CD25^+$ T cell-mediated suppression by dendritic cells. *Science* 299: 1033–1036.
41. Lyko, F., and R. Brown. 2005. DNA methyltransferase inhibitors and the development of epigenetic cancer therapies. *J. Natl. Cancer Inst.* 97: 1498–1506.
42. Egger, G., G. Liang, A. Aparicio, and P. A. Jones. 2004. Epigenetics in human disease and prospects for epigenetic therapy. *Nature* 429: 457–463.
43. Davidson, T. S., R. J. DiPaolo, J. Andersson, and E. M. Shevach. 2007. Cutting edge: IL-2 is essential for TGF-β-mediated induction of $Foxp3^+$ T regulatory cells. *J. Immunol.* 178: 4022–4026.
44. Tran, D. Q., H. Ramsey, and E. M. Shevach. 2007. Induction of FOXP3 expression in naive human $CD4^+$ FOXP3 T cells by T-cell receptor stimulation is transforming growth factor-β dependent but does not confer a regulatory phenotype. *Blood* 110: 2983–2990.
45. Piccirillo, C. A., J. J. Letterio, A. M. Thornton, R. S. McHugh, M. Mamura, H. Mizuhara, and E. M. Shevach. 2002. $CD4^+CD25^+$ regulatory T cells can mediate suppressor function in the absence of transforming growth factor β1 production and responsiveness. *J. Exp. Med.* 196: 237–246.

46. Fahlen, L., S. Read, L. Gorelik, S. D. Hurst, R. L. Coffman, R. A. Flavell, and F. Powrie. 2005. T cells that cannot respond to TGF-β escape control by $CD4^+CD25^+$ regulatory T cells. *J. Exp. Med.* 201: 737–746.
47. Liu, Y., P. Zhang, J. Li, A. B. Kulkarni, S. Perruche, and W. Chen. 2008. A critical function for TGF-βsignaling in the development of natural $CD4^+CD25^+Foxp3^+$ regulatory T cells. *Nat. Immunol.* 9: 632–640.
48. Tao, R., E. F. de Zoeten, E. Ozkaynak, C. Chen, L. Wang, P. M. Porrett, B. Li, L. A. Turka, E. N. Olson, M. I. Greene, et al. 2007. Deacetylase inhibition promotes the generation and function of regulatory T cells. *Nat. Med.* 13: 1299–1307.
49. Zorn, E., E. A. Nelson, M. Mohseni, F. Porcheray, H. Kim, D. Litsa, R. Bellucci, E. Raderschall, C. Canning, R. J. Soiffer, et al. 2006. IL-2 regulates FOXP3 expression in human $CD4^+CD25^+$ regulatory T cells through a STAT-dependent mechanism and induces the expansion of these cells in vivo. *Blood* 108: 1571–1579.
50. Wei, J., O. Duramad, O. A. Perng, S. L. Reiner, Y. J. Liu, and F. X. Qin. 2007. Antagonistic nature of T helper 1/2 developmental programs in opposing peripheral induction of $Foxp3^+$ regulatory T cells. *Proc. Natl. Acad. Sci. USA* 104: 18169–18174.
51. Mantel, P. Y., H. Kuipers, O. Boyman, C. Rhyner, N. Ouaked, B. Ruckert, C. Karagiannidis, B. N. Lambrecht, R. W. Hendriks, R. Crameri, et al. 2007. GATA3-driven Th2 responses inhibit TGF-β1-induced FOXP3 expression and the formation of regulatory T cells. *PLoS Biol.* 5: e329.
52. Zhang, Q., H. Y. Wang, A. Woetmann, P. N. Raghunath, N. Odum, and M. A. Wasik. 2006. STAT3 induces transcription of the DNA methyltransferase 1 gene (DNMT1) in malignant T lymphocytes. *Blood* 108: 1058–1064.
53. Zhang, Q., H. Y. Wang, M. Marzec, P. N. Raghunath, T. Nagasawa, and M. A. Wasik. 2005. STAT3- and DNA methyltransferase 1-mediated epigenetic silencing of SHP-1 tyrosine phosphatase tumor suppressor gene in malignant T lymphocytes. *Proc. Natl. Acad. Sci. USA* 102: 6948–6953.
54. Allan, S. E., S. Q. Crome, N. K. Crellin, L. Passerini, T. S. Steiner, R. Bacchetta, M. G. Roncarolo, and M. K. Levings. 2007. Activation-induced FOXP3 in human T effector cells does not suppress proliferation or cytokine production. *Int. Immunol.* 19: 345–354.
55. Smith, E. L., H. M. Finney, A. M. Nesbitt, F. Ramsdell, and M. K. Robinson. 2006. Splice variants of human FOXP3 are functional inhibitors of human $CD4^+$ T-cell activation. *Immunology* 119: 203–211.